

FORSCHUNGSZENTRUM KARLSRUHE

Technik und Umwelt

Wissenschaftliche Berichte

FZKA 6026

T-stresses for internally cracked components

T. Fett

Institut für Materialforschung

Forschungszentrum Karlsruhe GmbH, Karlsruhe

1997

T-stresses for internally cracked components

Abstract:

The failure of cracked components is governed by the stresses in the vicinity of the crack tip. The singular stress contribution is characterised by the stress intensity factor K , the first regular stress term is represented by the so-called T-stress.

T-stress solutions for components containing an internal crack were computed by application of the Boundary Collocation Method (BCM). The results are compiled in form of tables or approximative relations.

In addition a Green's function for T-stresses is proposed for internal cracks which enables to compute T-stress terms for any given stress distribution in the uncracked body.

T-Spannungen in Bauteilen mit Innenrissen

Kurzfassung:

Das Versagen von Bauteilen mit Rissen wird durch die unmittelbar an der Rispitze auftretenden Spannungen verursacht. Der singulre Anteil diese Spannungen wird durch den Spannungsintensittsfaktor K charakterisiert. Der erste regulre Term wird durch die sogenannte T-Spannung beschrieben.

Im vorliegenden Bericht werden Ergebnisse mitgeteilt, die mit der "Boundary Collocation Methode" (BCM) bestimmt wurden. Die Resultate werden in Form von Tabellen und Nherungsformeln wiedergegeben.

Zustzlich wird eine Greensfunktion fr Innenrisse angegeben. Diese erlaubt die Berechnung des T-Spannungsterms fr beliebige Spannungsverteilungen in der ungerissenen Struktur.

Contents

1	Introduction	1
2	T-stress term	2
3	Green's function for T-stress	4
3.1	Representation of T-stresses by a Green's function	4
3.2	Set-up for the Green's function	5
3.2.1	Asymptotic term	5
3.2.2	Correction terms for the Green's function	7
3.2.2.1	Edge cracks	7
3.2.2.2	Internal cracks	8
4	Boundary Collocation Procedure	10
4.1	Boundary conditions	10
4.2	Stress function for point forces	11
5	Results	14
5.1	Crack in an infinite body	14
5.1.1	Couples of forces	14
5.1.2	Constant crack face loading	15
5.2	Circular disk with internal crack	16
5.2.1	Constant internal pressure	16
5.2.2	Disk partially loaded by normal tractions	18
5.2.3	Central point force on the crack face	20

5.3 Rectangular plate with internal crack	23
6 Estimation of T-terms with a Green's function	26
6.1 Green's function with one regular term	26
6.2 Green's function with two regular terms	28
7 References	30
Appendix	32

1 Introduction

The fracture behaviour of cracked structures is dominated by the near-tip stress field. In fracture mechanics, interest focusses on stress intensity factors, which describe the singular stress field ahead of a crack tip and govern fracture of a specimen when a critical stress intensity factor is reached. Nevertheless, there is experimental evidence (e.g. [1-3]) that also the constant stress contributions acting over a longer distance from the crack tip may affect fracture mechanics properties. Sufficient information about the stress state is available, if the stress intensity factor and the constant stress term, the T-stress, are known.

While stress intensity factor solutions are reported in handbooks for many crack geometries and loading cases, T-stress solutions are available only for a small number of test specimens and simple loading cases as for instance pure tension and bending.

Different methods were applied in the past to compute the T-stress term for fracture mechanics standard test specimens. Regarding one-dimensional cracks, Leever and Radon [4] made a numerical analysis based on a variational method. Kfoury [5] applied the Eshelby technique. Sham [6,7] developed a second-order weight function based on a work-conjugate integral and evaluated it for the SEN specimen using the FE method. In [8,9] a Green's function for T-stresses was determined on the basis of Boundary Collocation results. Wang and Parks [10] extended the T-stress evaluation to two-dimensional surface cracks using the line-spring method.

In earlier reports the T-stress term for single edge-cracked structures [11] and for double-edge cracked plates [12] were communicated.

In the present report the computations are extended to internal one-dimensional cracks. Since the Boundary Collocation method provides T-stress terms as well as stress intensity factors, some stress intensity factor solutions will be reported.

2 T-stress term

The complete stress state in a cracked body is known if a related stress function is known. In most cases, the Airy stress function Φ is an appropriate tool which results as the solution of

$$\Delta\Delta\Phi = 0 \quad (2.1)$$

For a cracked body a series representation for Φ was given by Williams [13]. Its symmetric part can be written in polar coordinates with the crack tip as the origin

$$\begin{aligned} \Phi = \sigma^* W^2 \sum_{n=0}^{\infty} (r/W)^{n+3/2} A_n \left[\cos(n + \frac{3}{2})\varphi - \frac{n + \frac{3}{2}}{n - \frac{1}{2}} \cos(n - \frac{1}{2})\varphi \right] \\ + \sigma^* W^2 \sum_{n=0}^{\infty} (r/W)^{n+2} A_n^* [\cos(n+2)\varphi - \cos n\varphi] \end{aligned} \quad (2.2)$$

where σ^* is a characteristic stress and W is a characteristic dimension. The geometric data are explained by Fig. 2.1.

From this stress function the x-component of the stresses results at $\varphi=0$

$$\sigma_x / \sigma^* = -\sum_{n=0}^{\infty} A_n \left(\frac{a-x}{W} \right)^{n-1/2} \frac{(2n+3)(2n+1)}{2n-1} - \sum_{n=0}^{\infty} 4A_n^* \left(\frac{a-x}{W} \right)^n (n+1) \quad (2.3)$$

The term with coefficient A_0 is related to the stress intensity factor K_I by

$$K_I = \sigma^* F \sqrt{\pi a} \quad (2.4)$$

with the geometric function F

$$F = A_0 \sqrt{18/\alpha} \quad , \quad \alpha = a/W \quad (2.5)$$

The term with coefficient A_0^* represents the total constant σ_x -stress contribution appearing at the crack tip ($x=a$) of a cracked structure

$$\sigma_x \Big|_{x=a} = -4\sigma^* A_0^* \quad (2.6)$$

This total x-stress includes stress contributions which are already present at the location $x=a$ in the uncracked body, $\sigma_{x,a}^{(0)}$, and an additional stress term which is generated by the crack exclusively. This contribution of the crack is called the T-stress and given by

$$T = -4\sigma^* A_0^* - \sigma_{x,a}^{(0)} \quad (2.7)$$

The total x-stress component is also of interest for fracture mechanics considerations. This may give rise to defining an additional T-term, T', by

$$T' = T + \sigma_{x,a}^{(0)} = -4\sigma^* A^*_0 \quad (2.8)$$

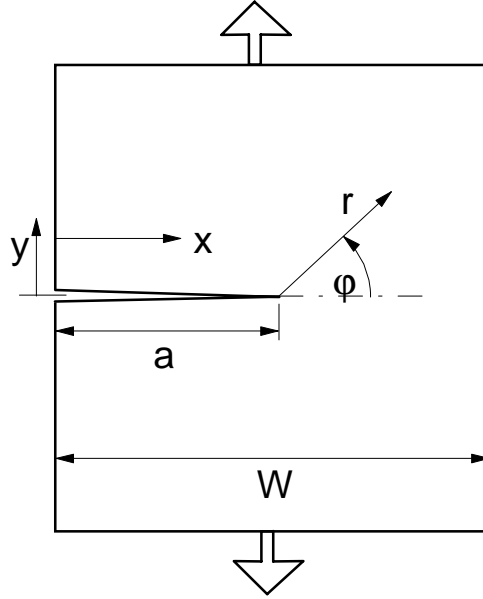


Fig. 1 Geometrical data of a crack in a component.

Leevers and Radon [4] proposed a dimensionless representation by the stress biaxiality ratio β

$$\beta = \frac{T\sqrt{\pi a}}{K_I} = \frac{T}{\sigma^* F} \quad (2.9)$$

Taking into consideration the singular stress term and the first regular term, the near-tip stress field can be described by

$$\sigma_{ij} = \frac{K_I}{\sqrt{2\pi a}} f_{ij}(\varphi) + \sigma_{ij,0} \quad (2.10)$$

$$\sigma_{ij,0} = \begin{pmatrix} \sigma_{xx,0} & \sigma_{xy,0} \\ \sigma_{yx,0} & \sigma_{yy,0} \end{pmatrix} = \begin{pmatrix} T & 0 \\ 0 & 0 \end{pmatrix} \quad (2.11)$$

where f_{ij} are the well-known angular functions for the singular stress contribution.

3 Green's function for T-stress

3.1 Representation of T-stresses by a Green's function

As a consequence of the principle of superposition, stress fields for different loadings can be added in the case of single loadings acting simultaneously. This leads to an integration representation of the loading parameters and was applied very early to the singular stress field and the computation of the related stress intensity factor by Bückner [14]. Similarly, the T-stress term can be expressed by an integral [6-9]. The integral representations read

$$K_I = \int_0^a h(x, a) \sigma_y(x) dx \quad , \quad T = \int_0^a t(x, a) \sigma_y(x) dx \quad (3.1)$$

where the integration has to be performed with the stress field σ_y in the uncracked body (Fig.2). The stress contributions are weighted by a weight function (h, t) dependent on the location x where the stress σ_y acts.

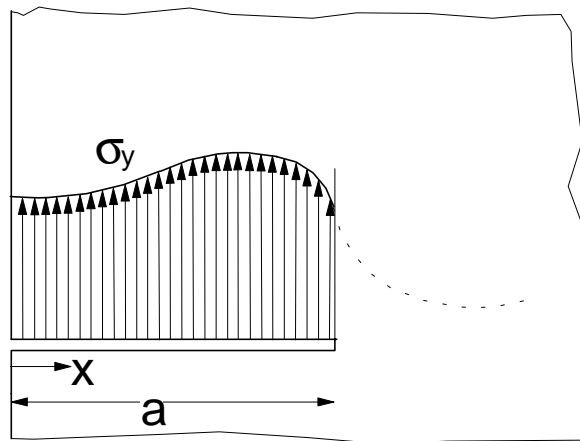


Fig. 2 Crack loaded by continuously distributed normal tractions.

The weight function can be interpreted as the stress intensity factor and as the T-term for a pair of single forces P acting at the crack face at the location x_0 (Fig.3), i.e. the weight functions (h, t) are Green's functions for K_I and T . This can be shown easily. The single forces are represented by a stress distribution

$$\sigma(x) = \frac{P}{B} \delta(x - x_0) \quad (3.2)$$

where δ is the Dirac Delta-function and B is the thickness of the plate (often chosen to be $B=1$). By introducing these stress distribution into (3.2) we obtain

$$K_P = \frac{P}{B} \int_0^a \delta(x - x_0) h(x, a) dx = \frac{P}{B} h(x_0, a) \quad (3.3a)$$

$$T_P = \frac{P}{B} \int_0^a \delta(x - x_0) t(x, a) dx = \frac{P}{B} t(x_0, a) \quad (3.3b)$$

i.e. the weight function terms $h(x_0, a)$ and $t(x_0, a)$ are the Green's functions for the stress intensity factor and T-stress term.

3.2 Set-up of the Green's function

3.2.1 Asymptotic term

In order to describe the Green's function, a separation is made consisting of a term t_0 representing the asymptotic limit case of near-tip behaviour and a correction term t_{corr} which includes information about the special shape of the component and the finite dimensions,

$$t = t_0 + t_{corr} \quad (3.4)$$

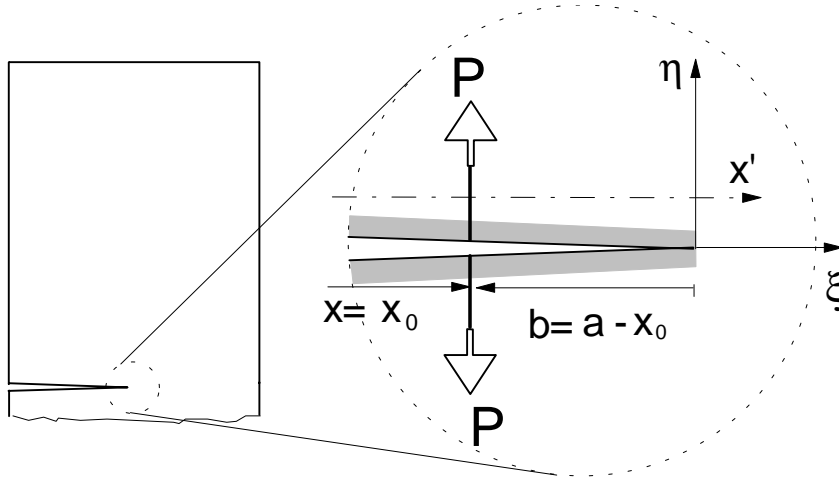


Fig. 3 Situation at the crack tip for asymptotic stress consideration.

In order to obtain information on the asymptotic behaviour of the weight or Green's function, we consider exclusively the near-tip behaviour. Therefore, we take into consideration a small section of the body (dashed circle) very close to the crack tip (Fig.3). The near-tip zone is

zoomed very strongly. Consequently, the outer borders of the component move to infinity. Now, we have the case of a semi-infinite crack in an infinite body. If we load the crack faces by a couple of forces P at location $x=x_0 \ll a$, the stress state can be described in terms of the Westergaard stress function [15]:

$$Z = \frac{P}{\pi} \frac{1}{z+b} \sqrt{\frac{b}{z}} \quad , \quad z = \xi + i\eta \quad (3.5)$$

The regular contribution to the stress function is ($z, b \neq 0$)

$$Z_{reg} = -\frac{P}{\pi} \frac{1}{z+b} \sqrt{\frac{z}{b}} \quad (3.6)$$

from which the regular part of the x-stress component results as

$$\sigma_x = \operatorname{Re} Z - y \operatorname{Im}(dZ/dz) \Rightarrow \sigma_x|_{y=0} = \operatorname{Re}\{Z\}|_{y=0} \quad (3.7)$$

$$\sigma_{x,reg}|_{y=0} = \operatorname{Re}\{Z_{reg}\}|_{y=0} = -\frac{P}{\pi} \frac{\sqrt{x'-a}}{(x'-x)\sqrt{a-x}} \quad , \quad x' > a \quad (3.8)$$

The constant x-stress term, i.e. the regular x-stress at $x'=0$ is then given by

$$\sigma_{x,reg}|_{x \rightarrow 0} = -\frac{P}{\pi} \lim_{x' \rightarrow a} \frac{\sqrt{x'-a}}{(x'-x)\sqrt{a-x}} \quad (3.9)$$

and the Green's function reads

$$\Rightarrow t_0 = -\frac{1}{\pi} \lim_{x' \rightarrow a} \frac{\sqrt{x'-a}}{(x'-x)\sqrt{a-x}} \quad (3.10)$$

From (3.9), the T-stress can be derived for a couple of forces for a semi-infinite crack in an infinite body, namely

$$T = \begin{cases} 0 & \text{for } x < a \\ \infty & \text{for } x = a \end{cases} \quad (3.11)$$

Let us consider the crack loading p to be represented by a Taylor series with respect to the crack tip as

$$p(x) = p|_{x=a} - \frac{dp}{dx}|_{x=a} (a-x) + \frac{1}{2} \frac{d^2p}{dx^2}|_{x=a} (a-x)^2 - \dots \quad (3.12)$$

The corresponding T-stress contribution, resulting from the asymptotic part of the Green's function, is given by

$$T_0 = \int_0^a t_0(x', a, x) \sigma(x) dx = -\frac{1}{\pi} \sigma_y \Big|_{x=a} \lim_{x' \rightarrow a} \sqrt{x'-a} \int_0^a \frac{dx}{(x'-x)\sqrt{a-x}} + R \quad (3.13)$$

with the remainder R containing integrals of the type

$$I_n = \int_0^a \frac{(a-x)^{n-1/2}}{x'-x} dx, \quad n \geq 1 \quad (3.14)$$

which yield (see e.g. integral 212.14a in [16])

$$I_n = 2 \sum_{\nu=0}^{n-1} \frac{(a-x')^\nu}{2n-1-2\nu} a^{n-\nu-1/2} + a^{n-1/2} \ln \frac{\sqrt{a}-\sqrt{x'-a}}{\sqrt{a}+\sqrt{x'-a}} \quad (3.15)$$

Consequently, the limit value is

$$\lim_{x' \rightarrow a} \sqrt{x'-a} I_n = 0 \Rightarrow R = 0 \quad (3.16)$$

and the term T_0 is exclusively represented by the first integral term in (3.13). Integration of this term results in

$$\begin{aligned} -\frac{1}{\pi} p \Big|_{x=a} \lim_{x' \rightarrow a} \sqrt{x'-a} \int_0^a \frac{dx}{(x'-x)\sqrt{a-x}} &= -\frac{1}{\pi} p \Big|_{x=a} \lim_{x' \rightarrow a} \sqrt{x'-a} \left[\frac{2}{\sqrt{x'-a}} \arctan \sqrt{\frac{x'-a}{a-x}} \right]_0^a = \\ &= -\frac{1}{\pi} p \Big|_{x=a} \lim_{x' \rightarrow a} \left[\pi - \arctan \sqrt{\frac{x'-a}{a}} \right] = -p \Big|_{x=a} \end{aligned} \quad (3.17)$$

$$\Rightarrow T_0 = -p \Big|_{x=a} = -\sigma_y \Big|_{x=a} \quad (3.18)$$

3.2.2 Correction terms for the Green's function

3.2.2.1 Edge cracks

By the considerations made before, only the asymptotic part of the x-stress is derived. Since a small region around the crack tip was chosen, the component boundaries were shifted to infinity. Now, a set-up has to be chosen for the weight function contribution t_{corr} which includes the finite size of the component.

Let us assume the difference between the complete Green's function $t(b)$ and its asymptotic part $t_0(b)$ to be expressible in a Taylor series for $b=a-x \rightarrow 0$

$$t_{corr}(b) = t(b) - t_0(b) = f(b) = 0 + \left. \frac{\partial t}{\partial b} \right|_{b=0} b + \frac{1}{2} \left. \frac{\partial^2 t}{\partial b^2} \right|_{b=0} b^2 + \dots \quad (3.19)$$

Then the complete Green's function can be written as

$$t = t_0 + \sum_{\nu=1}^{\infty} C_{\nu} (1 - x/a)^{\nu} \quad (3.20)$$

If we restrict the expansion to the leading term, we obtain as an approximation

$$t \cong t_0 + C \left(1 - \frac{x}{a} \right) \quad (3.21)$$

A simple procedure to determine approximative Green's functions is possible by determination of the unknown coefficients in the series representation (3.20) to known T-solutions for reference loading cases [9]. The general treatment may be shown for the determination of the coefficient C for an approximative weight function representation according to (3.21).

Let us assume the T-term T_t of a centrally cracked plate under pure tension σ_0 to be known. Introducing (3.21) into (3.1) yields

$$T = \sigma_0 \int_0^a t(x, a) dx = \sigma_0 \int_0^a t_0 dx + \sigma_0 C \int_0^a (1 - x/a) dx = \sigma_0 \left(-1 + C \frac{a}{2} \right) \quad (3.22)$$

and the coefficient C results as

$$C = \frac{2}{a} \left(1 + \frac{T_t}{\sigma_0} \right) \quad (3.23)$$

Knowledge of additional reference solutions for T allows to determine further coefficients.

3.2.2.2 Internal crack

The derivation of an approximate Green's function for internal cracks is similar to those of edge cracks. Due to the symmetry at $x=0$, the general set-up must be modified. An improved description that fulfills eq.(3.19) and is symmetric with respect to $x=0$ is

$$t = t_0 + \sum_{\nu=1}^{\infty} C_{\nu} (1 - x^2/a^2)^{\nu} \quad (3.24)$$

with the first approximation

$$t \cong t_0 + C(1 - x^2 / a^2) \quad (3.25)$$

In this case, the coefficient C results from the pure tension case as

$$C = \frac{3}{2a} \left(1 + \frac{T_t}{\sigma_0} \right) \quad (3.26)$$

4 Boundary Collocation Procedure

4.1 Boundary conditions

A simple possibility to determine the coefficients A_0 and A^*_0 is the application of the Boundary Collocation Method (BCM) [17-19]. For practical application of eq.(2), which is used to determine A_0 and A^*_0 , the infinite series for the Airy stress function must be truncated after the N th term for which an adequate value must be chosen. The still unknown coefficients are determined by fitting the stresses and displacements to the specified boundary conditions. The stresses result from the relations

$$\sigma_r = \frac{1}{r} \frac{\partial \Phi}{\partial r} + \frac{1}{r^2} \frac{\partial^2 \Phi}{\partial \varphi^2} \quad (4.1)$$

$$\sigma_\varphi = \frac{\partial^2 \Phi}{\partial r^2} \quad (4.2)$$

$$\tau_{r\varphi} = \frac{1}{r^2} \frac{\partial \Phi}{\partial \varphi} - \frac{1}{r} \frac{\partial^2 \Phi}{\partial r \partial \varphi} \quad (4.3)$$

The displacements read in terms of the Williams stress function

$$\begin{aligned} \frac{u_x}{\sigma^* W} &= \frac{1+\nu}{E} \sum_{n=0}^{\infty} A_n \left(\frac{r}{W} \right)^{n+1/2} \frac{2n+3}{2n-1} [(n+4\nu-\frac{5}{2}) \cos(n-\frac{1}{2})\varphi - (n-\frac{1}{2}) \cos(n+\frac{3}{2})\varphi] + \\ &+ \frac{1+\nu}{E} \sum_{n=0}^{\infty} A_n^* \left(\frac{r}{W} \right)^{n+1} [(n+4\nu-2) \cos n\varphi - (n+2) \cos(n+2)\varphi] \end{aligned} \quad (4.4)$$

$$\begin{aligned} \frac{v}{\sigma^* W} &= \frac{1+\nu}{E} \sum_{n=0}^{\infty} A_n \left(\frac{r}{W} \right)^{n+1/2} \frac{2n+3}{2n-1} [(n-\frac{1}{2}) \sin(n+\frac{3}{2})\varphi - (n-4\nu+\frac{7}{2}) \sin(n-\frac{1}{2})\varphi] + \\ &+ \frac{1+\nu}{E} \sum_{n=0}^{\infty} A_n^* \left(\frac{r}{W} \right)^{n+1} [(n+2) \sin(n+2)\varphi - (n-4\nu+4) \sin n\varphi] \end{aligned} \quad (4.5)$$

(ν =Poisson ratio), from which the needed Cartesian component results as

$$u_x = u \cos \varphi - v \sin \varphi \quad (4.6)$$

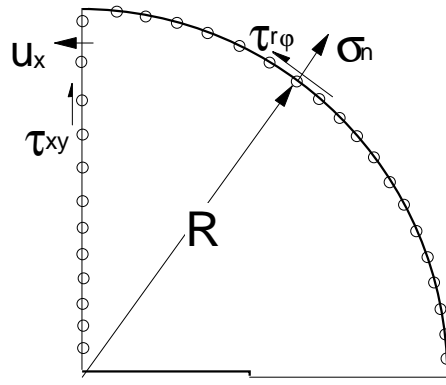


Fig. 4 Node selection and boundary conditions for an internally cracked disc.

In the special case of an internally cracked circular disc of radius R , the stresses at the boundaries are:

$$\sigma_n = \tau_{r\phi} = 0 \quad (4.7)$$

along the quarter circle. Along the perpendicular symmetry line, the boundary conditions are:

$$u_x = \text{const.} \rightarrow \frac{\partial u_x}{\partial y} = 0 \quad (4.8a)$$

$$\tau_{xy} = 0 \quad (4.8b)$$

About 100 coefficients for eq.(2) were determined from 600-800 stress and displacement equations at 400 nodes along the outer contour (symbolized by the circles in Fig. 4). For a selected number of $(N+1)$ collocation points, the related stress components (or displacements) are computed, and a system of $2(N+1)$ equations allows to determine up to $2(N+1)$ coefficients. The expenditure of computation can be reduced by the selection of a rather large number of edge points and by solving subsequently the then overdetermined system of equations using a least squares routine.

4.2 Stress function for point forces

The treatment of point forces at the crack face in case of a finite body is illustrated in the following sections for a circular disc with an internal crack loaded by a couple of forces at $x = y = 0$. In order to describe the crack-face loading by concentrated forces, we superimpose two loading cases. First, the singular crack-face loading is modelled by the centrally loaded crack in an infinite body described by the Westergaard stress function

$$Z = \frac{Pa}{\pi} \frac{1}{z\sqrt{z^2 - a^2}} \quad (4.9)$$

The stresses resulting from this stress function disappear only at infinite distances from the crack. In the finite body, consequently, the stress-free boundary condition is not fulfilled. To nullify the tractions at the outer boundaries, stresses resulting from the Airy stress function, eq.(2.2), are added which do not superimpose additional stresses at the crack faces. The basic principle used for such calculations, the principle of superposition, is illustrated in more detail in the Appendix.

The stresses caused by Z are

$$\sigma_x = \text{Re } Z - y \text{Im } Z' \quad (4.10)$$

$$\sigma_y = \text{Re } Z + y \text{Im } Z' \quad (4.11)$$

$$\tau_{xy} = -y \text{Re } Z' \quad (4.12)$$

with

$$Z' = \frac{dZ}{dz} = -\frac{Pa}{\pi} \frac{2z^2 - a^2}{z^2(z^2 - a^2)^{3/2}} \quad (4.13)$$

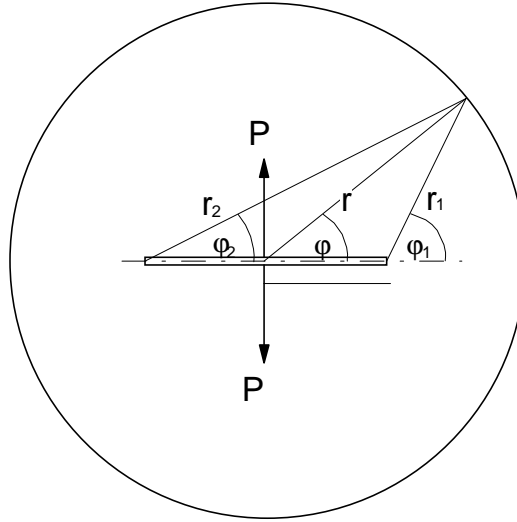


Fig. 5 Coordinate system for the application of the Westergaard stress function to a finite component.

For practical use it is of advantage to introduce the coordinates shown in Fig.5. The following geometric relations hold

$$z = r \exp(i\varphi), \quad z - a = r_1 \exp(i\varphi_1), \quad z + a = r_2 \exp(i\varphi_2) \quad (4.14)$$

$$r = \sqrt{x^2 + y^2}, \quad \tan \varphi = y / x \quad (4.15a)$$

$$r_1 = \sqrt{(x-a)^2 + y^2}, \quad \tan \varphi_1 = y / (x-a) \quad (4.15b)$$

$$r_2 = \sqrt{(x+a)^2 + y^2}, \quad \tan \varphi_2 = y / (x+a) \quad (4.15c)$$

$$\operatorname{Re} Z = \frac{Pa}{\pi r \sqrt{r_1 r_2}} \cos(\varphi + \frac{1}{2} \varphi_1 + \frac{1}{2} \varphi_2) \quad (4.16a)$$

$$\operatorname{Im} Z = -\frac{Pa}{\pi r \sqrt{r_1 r_2}} \sin(\varphi + \frac{1}{2} \varphi_1 + \frac{1}{2} \varphi_2) \quad (4.16b)$$

$$\operatorname{Re} Z' = -\frac{Pa}{\pi} \left[\frac{2}{(r_1 r_2)^{3/2}} \cos \frac{3}{2}(\varphi_1 + \varphi_2) - \frac{a^2}{r^2 (r_1 r_2)^{3/2}} \cos(2\varphi + \frac{3}{2} \varphi_1 + \frac{3}{2} \varphi_2) \right] \quad (4.16c)$$

$$\operatorname{Im} Z' = \frac{Pa}{\pi} \left[\frac{2}{(r_1 r_2)^{3/2}} \sin \frac{3}{2}(\varphi_1 + \varphi_2) - \frac{a^2}{r^2 (r_1 r_2)^{3/2}} \sin(2\varphi + \frac{3}{2} \varphi_1 + \frac{3}{2} \varphi_2) \right] \quad (4.16d)$$

The stress function Z provides no T-stress term as will be shown in 5.5.5. Nevertheless, the equilibrium tractions at the circumference act as a normal external load and may produce a T-stress. Radial and tangential stress components along the contour of the disc for a crack with $a/R=0.4$ are plotted in Fig.6.

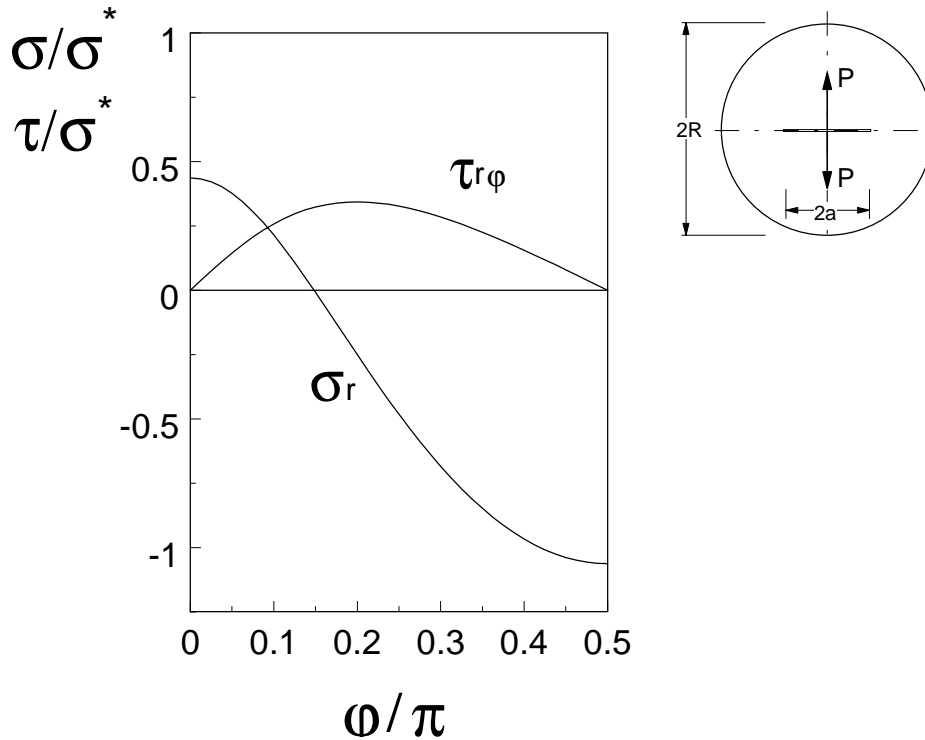


Fig.6 Normal and shear tractions created by the stress function (4.9) along the fictitious disc contour (for φ see Fig. 5), $\sigma^*=P/(\pi R)$.

5 Results

5.1 Crack in an infinite body

5.1.1 Couples of forces

The T-stress term resulting from a couple of symmetric point forces (see Fig.7) can be derived from the Westergaard stress function [15] which for this special case reads

$$Z = \frac{2P}{\pi} \frac{\sqrt{a^2 - x^2}}{(z^2 - x^2)\sqrt{1 - (a/z)^2}} \quad (5.1)$$

(note that eq.(3.5) is the limit of this relation for $x \rightarrow a$). The real part of (5.1) gives the x-stress component for $y = 0$

$$\sigma_x|_{y=0} = \text{Re}\{Z\} = \frac{2P}{\pi} \frac{\sqrt{a^2 - x^2} x'}{(x'^2 - x^2)\sqrt{x'^2 - a^2}} \quad (5.2)$$

Its singular part

$$\sigma_{x,\text{sing}}|_{y=0} = \frac{2P}{\pi} \frac{\sqrt{a/2}}{\sqrt{a^2 - x^2} \sqrt{x' - a}} \quad (5.3)$$

provides the well-known stress intensity factor solution

$$K = \lim_{x' \rightarrow a} \sqrt{2\pi(x' - a)} \sigma_x = \sqrt{\frac{a}{\pi}} \frac{2P}{\sqrt{a^2 - x^2}} \quad (5.4)$$

Then, the regular stress term reads

$$\sigma_{x,\text{reg}}|_{y=0} = \frac{2P}{\pi} \frac{(a^2 - x^2)x' - \sqrt{a/2}(x'^2 - x^2)\sqrt{x' + a}}{(x'^2 - x^2)\sqrt{x'^2 - a^2} \sqrt{a^2 - x^2}} \quad (5.5)$$

and for the T-stress term it results

$$T = \lim_{x' \rightarrow a} \sigma_{x,\text{reg}} = \begin{cases} 0 & \text{for } x < a \\ \infty & \text{for } x = a \end{cases} \quad (5.6)$$

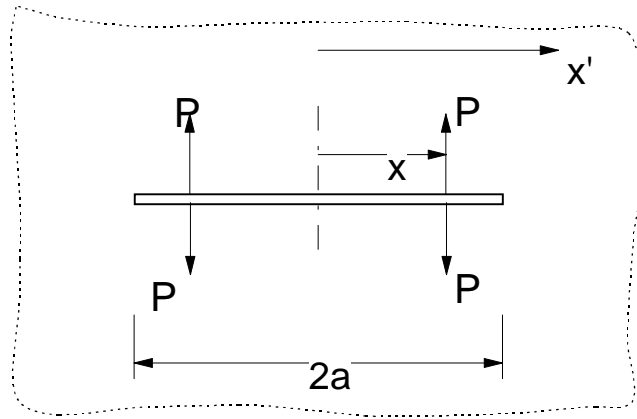


Fig. 7 Crack in an infinite body loaded by symmetric couples of forces.

5.1.2 Constant crack-face loading

In the case of a constant crack-face pressure $p = \text{const.}$ (Fig. 8), the stress function reads

$$Z = p \left[\frac{z}{\sqrt{z^2 - a^2}} - 1 \right] \quad (5.7)$$

resulting in the x-stress of

$$\sigma_x|_{y=0} = p \left[\frac{x'}{\sqrt{x'^2 - a^2}} - 1 \right] \quad (5.8)$$

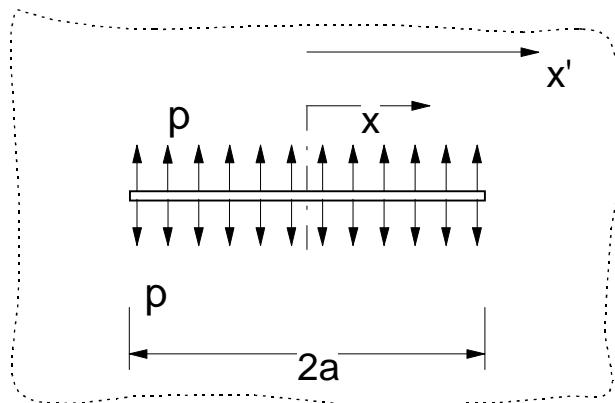


Fig. 8 Crack in an infinite body under constant crack-face pressure.

The T-stress term results as

$$T = -p \quad (5.9)$$

as found for the small-scale solution (3.18).

5.2 Circular disc with internal crack

5.2.1 Constant internal pressure

The crack under constant internal pressure (Fig. 9) has been analyzed with the Boundary Collocation method. T-stress and stress intensity factor (represented by the geometric function F) are shown in Fig. 10 and Table 1.

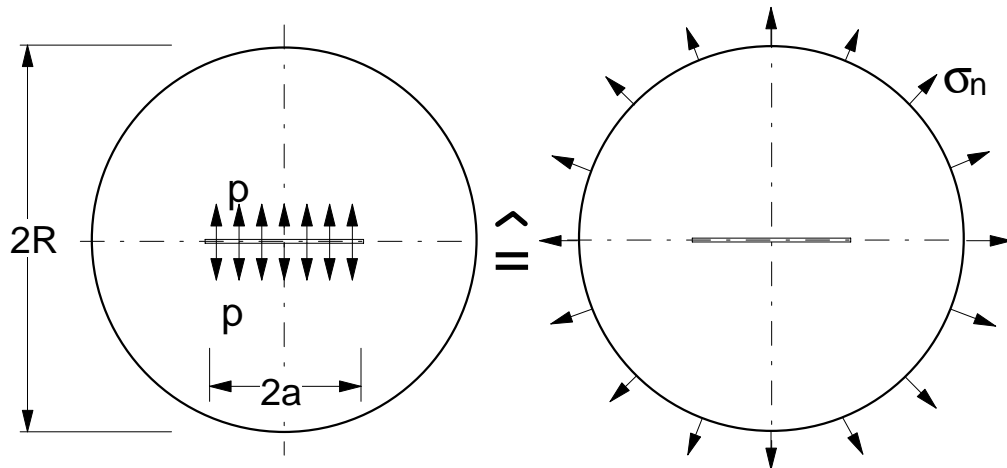


Fig. 9 Circular disc with internal crack under constant pressure p and equivalent problem of disc loading by normal tractions at the circumference.

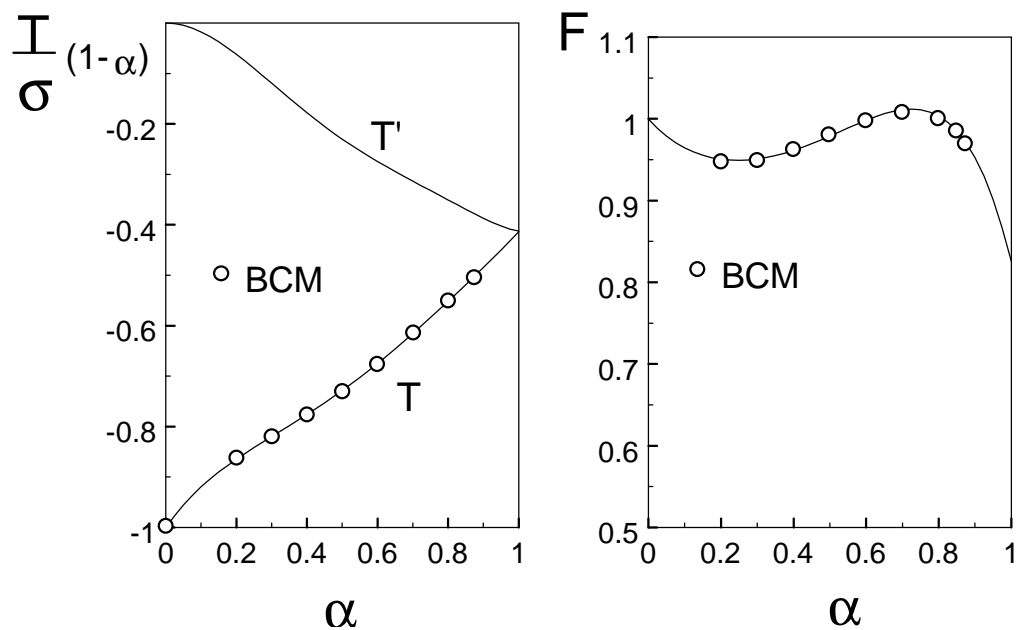


Fig. 10 T-stress and geometric function F for the stress intensity factor for an internal crack in a circular disc.

$\alpha = a/R$	$T/\sigma \cdot (1-\alpha)$	$T'/\sigma \cdot (1-\alpha)$	$F \cdot (1-\alpha)^{1/2}$	$\beta \cdot (1-\alpha)^{1/2}$
0	-1.00	0.000	1.000	-1.00
0.1	-0.919	-0.019	0.965	-0.952
0.2	-0.864	-0.064	0.951	-0.909
0.3	-0.820	-0.120	0.951	-0.862
0.4	-0.776	-0.176	0.962	-0.807
0.5	-0.728	-0.228	0.979	-0.744
0.6	-0.675	-0.275	0.998	-0.676
0.7	-0.615	-0.315	1.011	-0.608
0.8	-0.552	-0.352	1.004	-0.550
0.9	-0.485	-0.385	0.953	-0.509
1.0	-0.413	-0.413	0.8255	-0.50

Table 1 T-stress and stress intensity factor for an internally cracked circular disc with constant crack-face pressure (value T for $\alpha=1$ extrapolated); for T and T' see eqs.(2.7) and (2.8).

The T-values in Table 1 were extrapolated to $\alpha=1$. Within the numerical accuracy of the extrapolation, the limit values are

$$\lim_{\alpha \rightarrow 1} T / \sigma * (1 - \alpha) = \lim_{\alpha \rightarrow 1} T' / \sigma * (1 - \alpha) \cong -0.413 = -\frac{1}{\sqrt{\pi^2 - 4}} \quad (5.10)$$

and for the stress intensity factor limits the well-known values

$$\lim_{\alpha \rightarrow 1} F / \sigma * \sqrt{1 - \alpha} = \frac{2}{\sqrt{\pi^2 - 4}} \quad (5.11)$$

are entered. For the biaxiality ratio it results

$$\lim_{\alpha \rightarrow 1} \beta \sqrt{1 - \alpha} \cong \frac{1}{2} \quad (5.12)$$

The T-stress terms can be approximated by

$$T / \sigma = \frac{-1 + \alpha - 2.34 \alpha^2 + 4.27 \alpha^3 - 3.326 \alpha^4 + 0.9824 \alpha^5}{1 - \alpha} \quad (5.13)$$

$$T' / \sigma = \frac{-2.34 \alpha^2 + 4.27 \alpha^3 - 3.326 \alpha^4 + 0.9824 \alpha^5}{1 - \alpha} \quad (5.14)$$

The stress intensity factor solution is in good agreement with the geometric function [9]

$$F = \frac{1 - 0.5\alpha + 1.6873\alpha^2 - 2.671\alpha^3 + 3.2027\alpha^4 - 1.8935\alpha^5}{\sqrt{1-\alpha}} \quad (5.15)$$

which represents the numerical data of Fig. 10 within maximum deviations of 0.5%.

5.2.2 Disc partially loaded by normal tractions

A partially loaded disc is shown in Fig.11a. Constant normal tractions σ_n are applied at the circumference within an angle of 2γ .

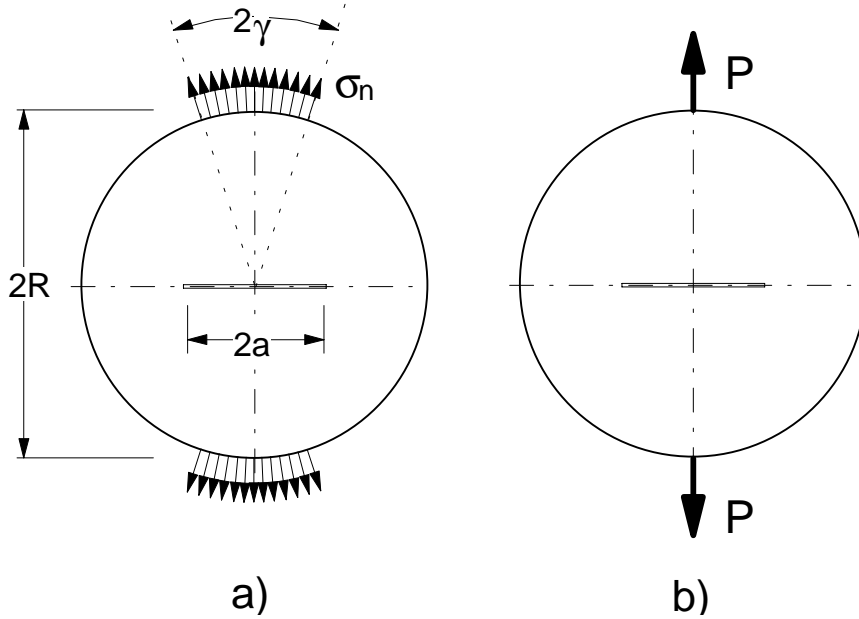


Fig. 11 a) partially loaded disc, b) diametral loading by a couple of forces.

The total force in y-direction results from

$$P_y = 2\sigma_n \int_0^\gamma R \cos \gamma' d\gamma' = 2\sigma_n R \sin \gamma \quad (5.16)$$

As a first result the stress intensity factor is obtained. The geometric function F , defined by

$$K_I = \sigma^* \sqrt{\pi a} F(a/R) , \quad \sigma^* = \frac{P_y}{\pi R} \quad (5.17)$$

is plotted in Fig. 12a. The x-stress term T , normalised to σ^* , is shown in Fig. 12b.

From the limit case $\gamma \rightarrow 0$, the solutions for concentrated forces (see Fig. 11b) are obtained as represented in Fig. 13. A comparison with the results from literature [20-22] gives good agreement in stress intensity factors. The solution given by Tada et al. [23] (dashed curve in Fig. 13a) deviates by about 20% near $a/R=0.8$. The results obtained here can be expressed by

$$K_I = \sigma^* \sqrt{\pi a} F_p, \quad F_p = \frac{3 - 1.254\alpha - 1.7013\alpha^2 + 4.0597\alpha^3 - 2.8059\alpha^4}{\sqrt{1-\alpha}} \quad (5.18)$$

with σ^* given in (5.16).

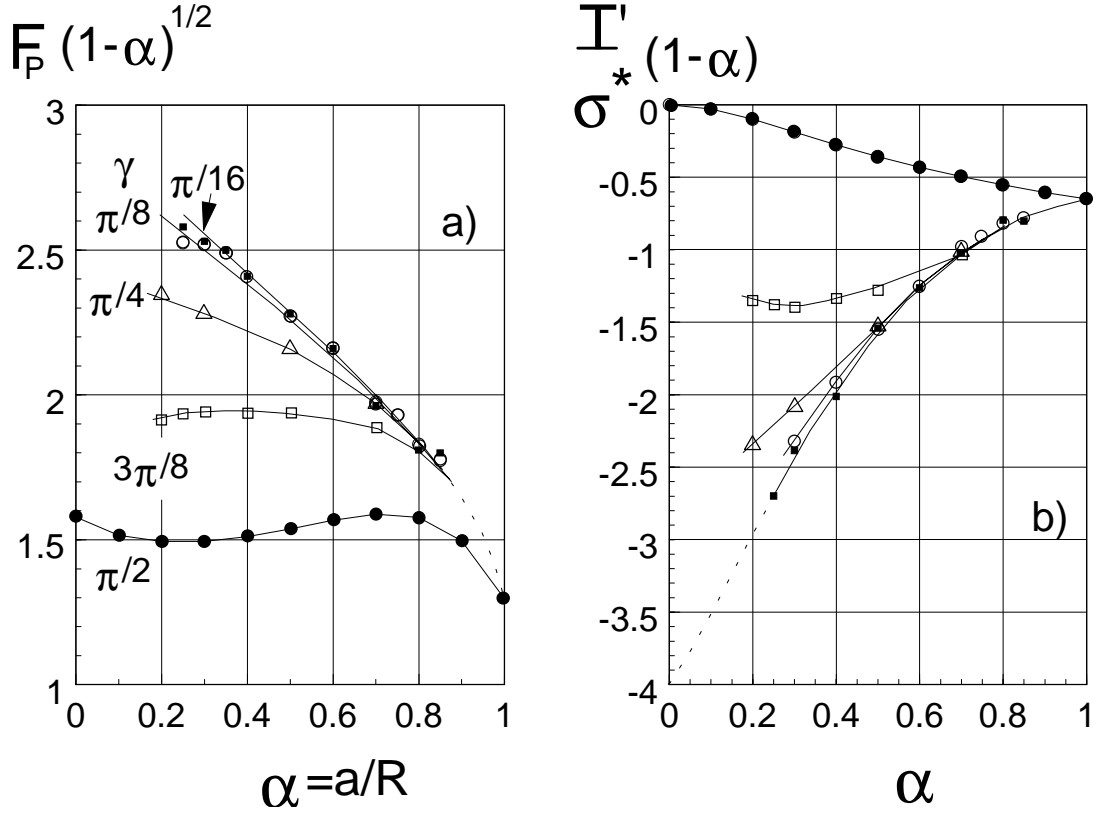


Fig. 12 Stress intensity factors and T-stress for a circular disc, partially loaded over an angle of 2γ (see Fig. 11a).

The T-stress T' can be fitted by

$$\frac{T'}{\sigma^*} = \frac{-4(1-\alpha) + 7.6777\alpha^2 - 16.0169\alpha^3 + 8.7994\alpha^4 - 1.10849\alpha^5}{1-\alpha} \quad (5.19)$$

Since the stresses in the uncracked disc under diametral loading by the couple of forces P are

$$\frac{\sigma_y}{\sigma^*} = \frac{4}{(1+\xi^2)^2} - 1, \quad \frac{\sigma_x}{\sigma^*} = -1 + \frac{4\xi^2}{(1+\xi^2)^2}, \quad \xi = x/R \quad (5.20)$$

with σ^* defined in (5.17), T can be computed from T'

$$\frac{T}{\sigma^*} = \frac{-3(1-\alpha) + 7.6777\alpha^2 - 16.0169\alpha^3 + 8.7994\alpha^4 - 1.10849\alpha^5}{1-\alpha} - \frac{4\alpha^2}{(1+\alpha^2)^2} \quad (5.21)$$

or expressed by a fit relation

$$\frac{T}{\sigma^*} \cong \frac{-3(1-\alpha) + 2.8996\alpha^2 - 6.1759\alpha^3 + 2.5438\alpha^4 + 0.0841\alpha^5}{1-\alpha} \quad (5.22)$$

In this case, the limit values are (at least in very good approximation)

$$\lim_{\alpha \rightarrow 1} T / \sigma^* (1 - \alpha) = \lim_{\alpha \rightarrow 1} T' / \sigma^* (1 - \alpha) \cong -0.648 \cong -\frac{\pi}{2\sqrt{\pi^2 - 4}} \quad (5.23)$$

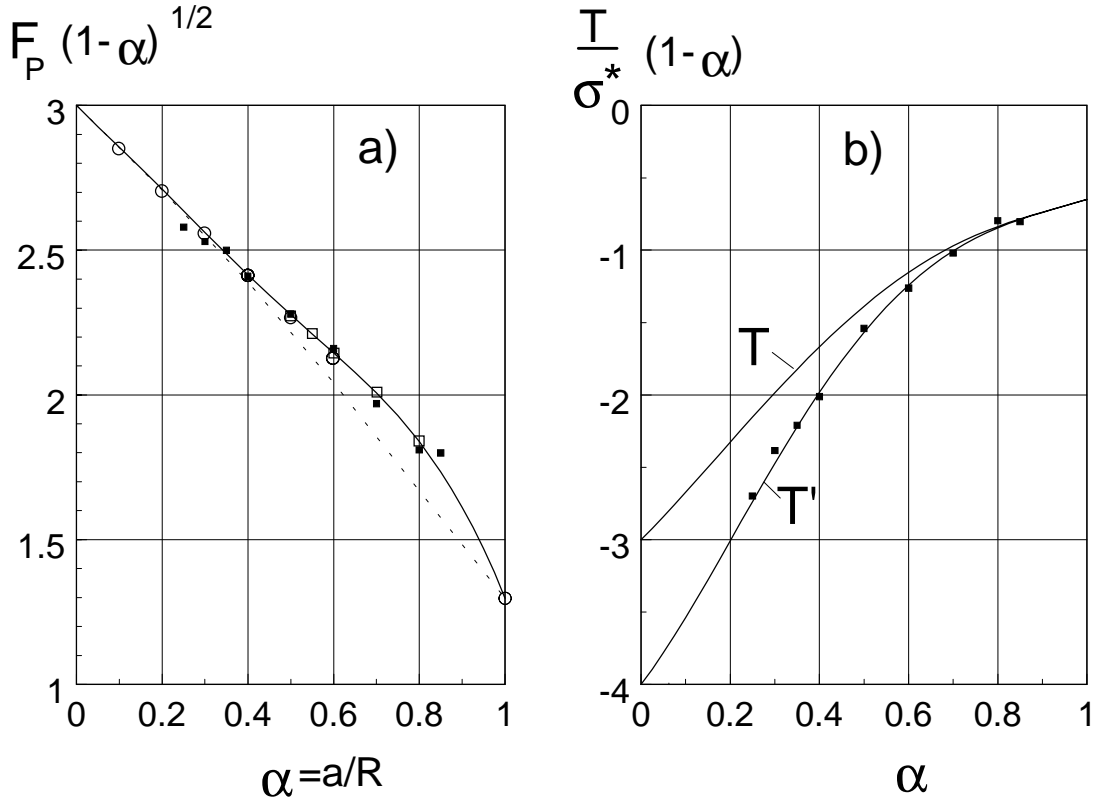


Fig. 13 Stress intensity factor and T-stress for a circular disc loaded diametrically by concentrated forces (Fig. 11b). a) Comparison of stress intensity factors; solid squares: partially distributed stresses with an angle of $\gamma=\pi/16$, circles: results by Atkinson et al. [20] and Awaji and Sato [21], open squares: results obtained with the weight function technique [22], dashed line: solution proposed by Tada et al.[23]. b) T-stress results: including partially distributed stresses with an angle of $\gamma=\pi/16$ (squares), and exact limit cases for $\alpha=0$.

5.2.3 Central point force on the crack face

A centrally cracked circular disc, loaded by a couple of forces at the crack center, is shown in Fig.14. For it, the stress intensity factors and T-stress were computed. Boundary Collocation computations dealing with the loading case of Fig.9 provide a set of coefficients A_n , from which the crack opening displacements (under constant crack-face pressure) result at $x=0$ [9]

$$u_y = \frac{1}{E'} \sum_{n=0}^N A_n a^{n+1/2} 4 \frac{2n+3}{2n-1} (-1)^{n+1} \quad (5.24)$$

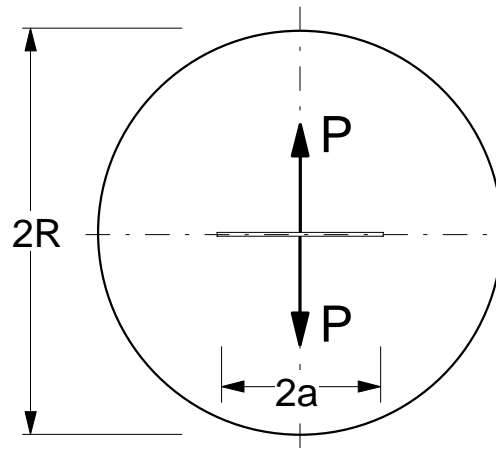


Fig. 14 Circular disc with a couple of forces acting on the crack faces.

The numerical data obtained with (5.24) can be represented in the whole range $0 \leq \alpha \leq 1$ by the fit relation

$$u_y = \frac{2pa}{E'} \left[-0.071 - 0.74188\alpha + 2.3041\alpha^2 - 2.3579\alpha^3 - \frac{1.071}{\alpha} \ln(1-\alpha) \right] \quad (5.25)$$

From the relation between the crack opening and weight function derived by Rice and by using the equivalence between the weight function and Green's function for stress intensity factors, the geometric function for the point forces, defined by

$$K_I = \frac{P}{\sqrt{\pi a}} F_p \quad (5.26)$$

is obtained as shown by the solid curve in Fig. 15. The description by a fit relation reads e.g.

$$F_p = \frac{1 - 1.07884\alpha + 8.24956\alpha^2 - 17.9026\alpha^3 + 20.3339\alpha^4 - 9.305\alpha^5}{\sqrt{1-\alpha}} \quad (5.27)$$

In addition Fig. 15 represents results obtained with further methods. Since the stress intensity factor at the crack center is directly related by the weight function at this location, application of the weight function reported in [9] yields the open circles. In this context it should be mentioned that the applied weight function was not derived from crack opening displacements, but by direct adjusting to two reference stress intensity factor solutions. The procedure described in Section 4.2 provides the data represented by squares.

Finally, the dashed curve represents a solution proposed by Tada et al. [23] based on an asymptotic estimation procedure.

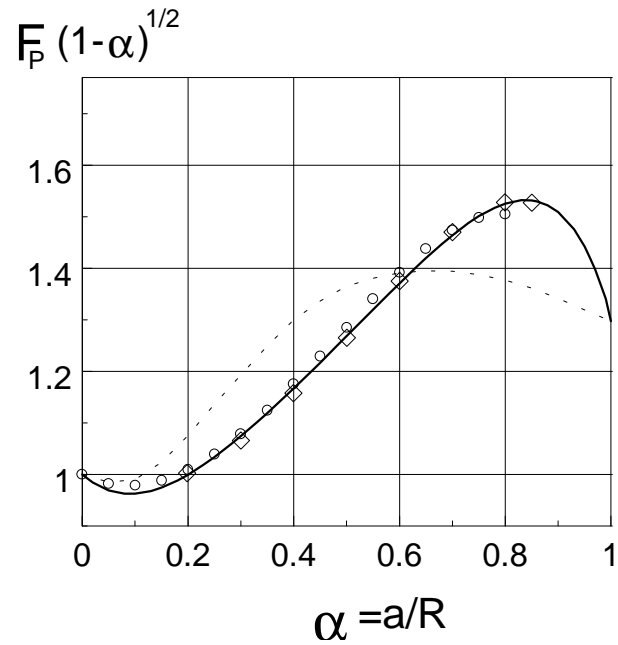


Fig. 15 Stress intensity factor for a couple of forces P at the crack center, represented by the geometric function F_P . Solid curve: derived from crack opening displacements at $x = 0$ using the Rice equation; open circles: obtained from the weight function [9]; squares: direct application of the Westergaard stress function for a crack in an infinite body superimposed with the Airy stress function describing the equilibrium tractions at the free disc boundary; dashed curve: Tada et al. [23].

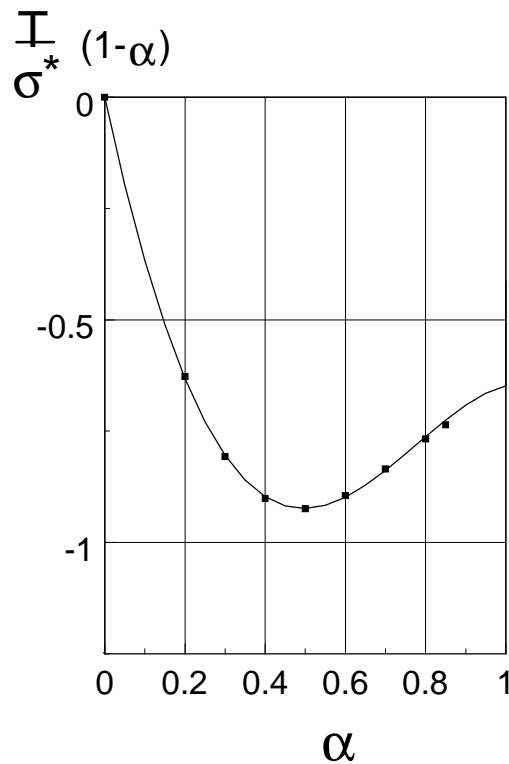


Fig. 16 T-stress for an internally cracked circular disc with a couple of forces acting in the crack center on the crack faces. Symbols: Numerical results, solid line: fitting curve.

The T-stress data obtained with the BCM-method according to Section 4.2 are plotted in Fig. 16 as squares. Together with this limit value the numerically found T-values were fitted by

$$\frac{T}{\sigma^*} = \frac{-4.1971\alpha + 5.4661\alpha^2 - 1.1497\alpha^3 - 0.7677\alpha^4}{1 - \alpha} \quad (5.28)$$

This relation is introduced into Fig. 16 as the solid line.

5.3 Rectangular plate with internal crack

The geometric data of the rectangular plate with an internal crack are illustrated in Fig.17.

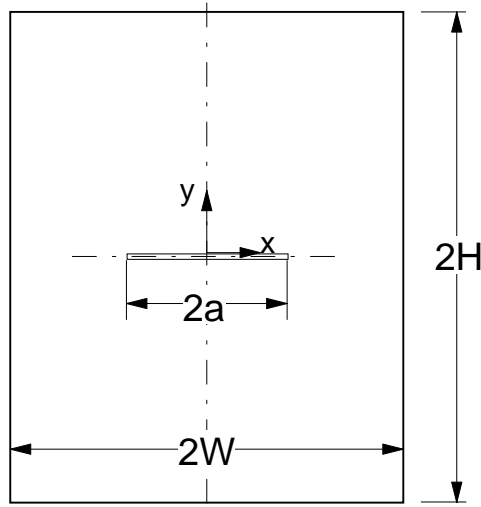


Fig. 17 Rectangular plate with a central internal crack (geometric data).

5.3.1 T-stress for pure tensile load

The plate under uniaxial load (tensile stresses exclusively at the ends $y = \pm H$) shows no σ_x -component in the uncracked structure. Consequently, the quantities T and T' are identical. T-stress results obtained by BCM-computations are shown in Fig. 18a and entered into Table 2. The biaxiality ratio, defined by eq.(2.9), is plotted in Fig. 18b and additionally given in Table 3.

For a long plate ($H/W > 1.5$) the biaxiality ratio β can be expressed by

$$\beta \cong -\frac{1 - 0.5\alpha}{\sqrt{1 - \alpha}} \quad (5.29)$$

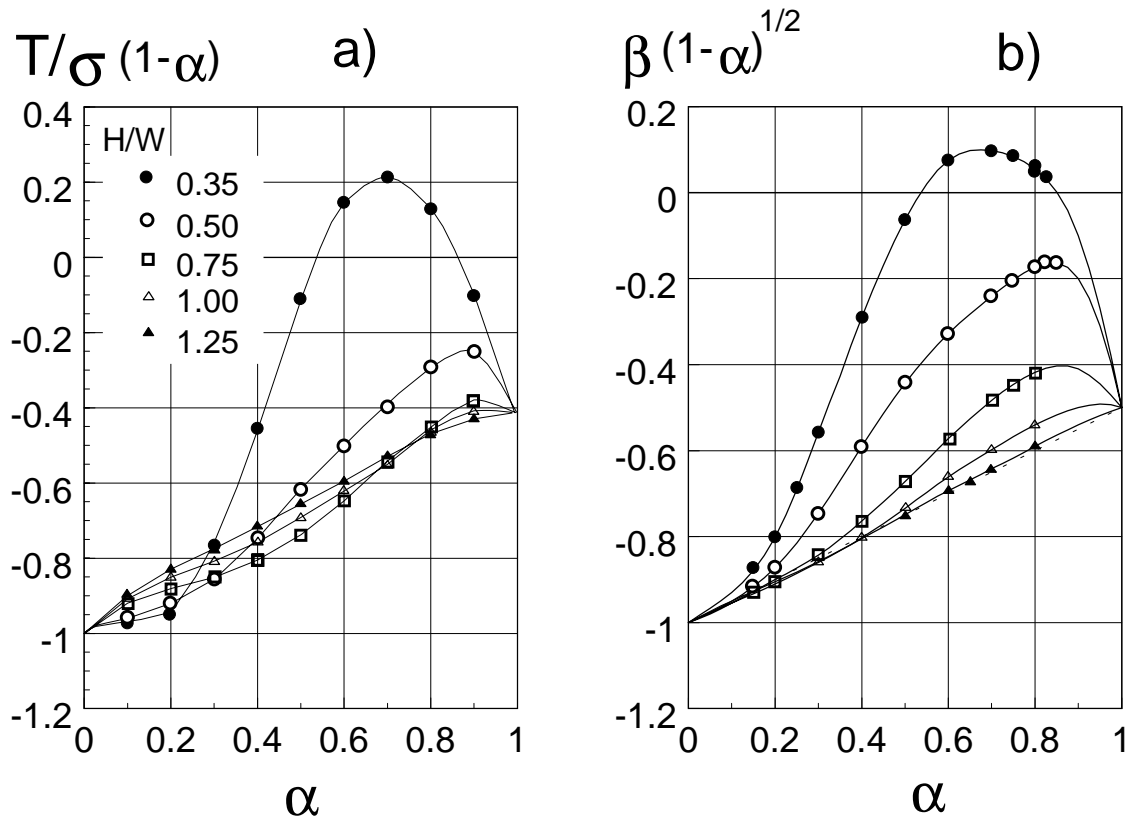


Fig.18 Internal crack in rectangular plate, a) T-stress, b) biaxiality ratio.

$\alpha = a/W$	$H/W=0.35$	0.50	0.75	1.00	1.25
0	-1.0	-1.0	-1.0	-1.0	-1.0
0.1	-0.97	-0.96	-0.92	-0.91	-0.9
0.2	-0.95	-0.92	-0.88	-0.85	-0.83
0.3	-0.766	-0.855	-0.85	-0.809	-0.777
0.4	-0.455	-0.745	-0.805	-0.756	-0.716
0.5	-0.110	-0.616	-0.738	-0.692	-0.656
0.6	0.145	-0.502	-0.647	-0.620	-0.596
0.7	0.215	-0.400	-0.543	-0.55	-0.53
0.8	0.13	-0.291	-0.45	-0.46	-0.47
0.9	-0.10	-0.25	-0.38	-0.41	-0.43
1.0	-0.413	-0.413	-0.413	-0.413	-0.413

Table 2 T-stress term, normalized as $T/\sigma(1-\alpha)$, for different crack and plate geometries.

$\alpha = a/W$	$H/W=0.35$	0.50	0.75	1.00	1.25
0	-1.0	-1.0	-1.0	-1.0	-1.0
0.1	-0.93	-0.95	-0.955	-0.955	-0.95
0.2	-0.801	-0.872	-0.90	-0.91	-0.905
0.3	-0.558	-0.746	-0.843	-0.860	-0.858
0.4	-0.291	-0.591	-0.764	-0.803	-0.805
0.5	-0.063	-0.443	-0.672	-0.734	-0.749
0.6	0.075	-0.328	-0.573	-0.661	-0.693
0.7	0.098	-0.241	-0.483	-0.598	-0.645
0.8	0.055	-0.173	-0.418	-0.54	-0.59
0.9	-0.1	-0.2	-0.41	0.5	-0.54
1.0	-0.5	-0.5	-0.5	-0.5	-0.5

Table 3 Biaxiality ratio, normalized as $\beta (1-\alpha)^{1/2}$, for different crack and plate geometries.

6 Estimation of T-terms with a Green's function

6.1 Green's function with one regular term

In order to estimate T-stresses, an approximate Green's function according to eqs.(3.25) and (3.26) may be applied. A Green's function with only one term was derived according to Section 3.2.3 using the case of constant crack-face pressure σ_0 as the reference loading case. In this rough approximation the T-term results as

$$T = C \int_0^a (1 - x^2 / a^2) \sigma(x) dx \quad , \quad C = \frac{3}{2a} \left(1 + \frac{T_\sigma}{\sigma_0} \right) \quad (6.1)$$

This section now deals with a check of the accuracy of the approximate Green's function by comparing the results of the set-up (3.25) with T-stress solutions found by application of the Boundary Collocation procedure.

First, the case of concentrated forces at $x=0$ (see Fig. 14) is considered. The couple of central forces reads in terms of the Dirac δ -function ($B=1$)

$$\sigma(x) = \frac{P}{2} \delta(x) \quad (6.2)$$

Introducing this and (5.13) into (6.1) leads to

$$T \approx \frac{3P}{4a} \left(1 + \frac{T_\sigma}{\sigma_0} \right) \quad (6.3)$$

$$\frac{T}{\sigma^*} \approx \frac{3\pi}{4} \frac{-2.34\alpha + 4.27\alpha^2 - 3.326\alpha^3 + 0.9824\alpha^4}{1-\alpha} \quad , \quad \sigma^* = \frac{P}{R\pi} \quad (6.4)$$

The result is plotted in Fig. 19.

As a second example, the diametral tension test is considered (see Fig. 11b). Introducing the stress distribution for a diametral tension test, eq.(5.20), into (6.1) yields, after numerical integration, the T-stress shown in Fig. 20.

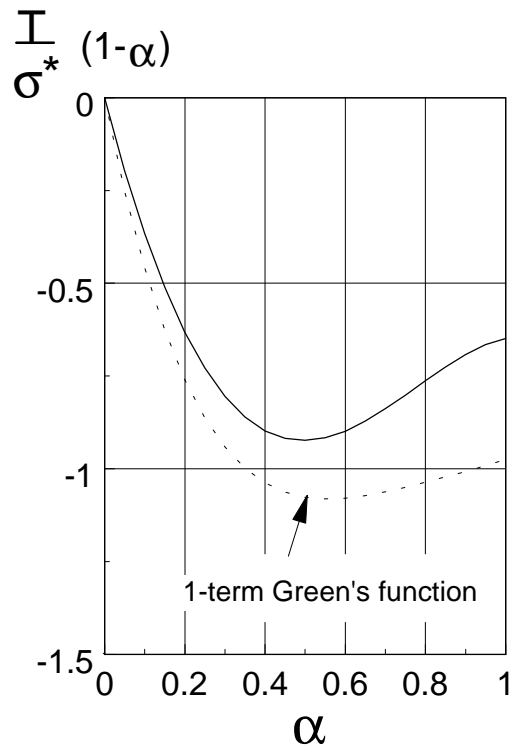


Fig. 19 T-stresses for an internally cracked circular disc, loaded by a couple of forces at the crack faces (see Fig. 14) estimated with a 1-term Green's function (dashed curve) compared with results from BCM-computations (solid curve).

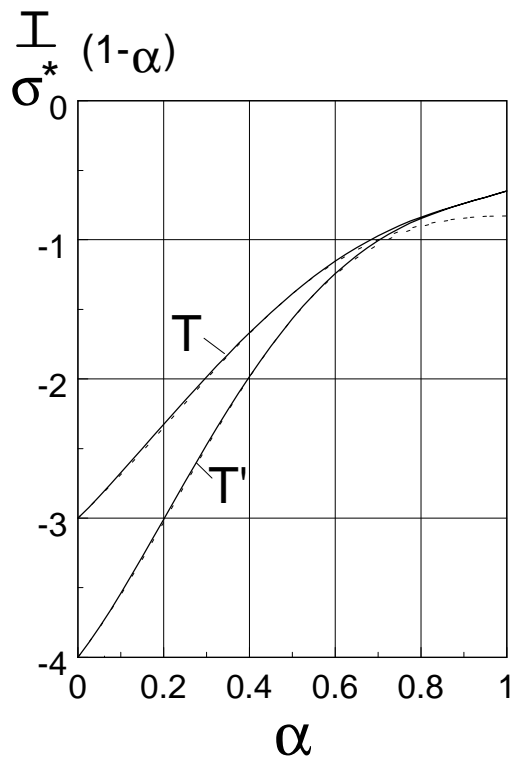


Fig. 20 T-stresses for an internally cracked circular disc, loaded by a couple of diametral forces at the free boundary (see Fig. 11b) estimated with a 1-term Green's function (dashed curve) compared with results from BCM-computations (solid curve).

From these two examples we can conclude for this first degree of approximation that the application to continuously distributed stresses gives significantly better results than the application to strongly non-homogeneous stresses as in the case of single forces at the crack faces. The reason for this behaviour is the fact that in the reference loading case (constant crack-face pressure) the load was also distributed homogeneously. In both cases the deviations increase with increasing relative crack size α . This makes evident that the Green's function needs higher order terms for larger α .

6.2 Green's function with two regular terms

In order to improve the Green's function, the next regular term is added. Consequently, the Green's function expansion reads

$$t = t_0 + C_1(1 - x^2 / a^2) + C_2(1 - x^2 / a^2)^2 \quad (6.5)$$

As a second reference loading case we now use the solution T_P for the internally cracked disc with a pair of single forces P at the crack center (see Fig. 14).

Introducing the two reference stresses

$$\sigma_1 = \text{const.} \quad \sigma_2 = \frac{P}{2} \delta(x) \quad (6.6)$$

into eq.(3.1) and carrying out the integration provides a system of two equations

$$T_1 / \sigma_1 = -1 + \frac{2a}{3} C_1 + \frac{8a}{15} C_2 \quad (6.7a)$$

$$T_2 / \sigma^* = \frac{\pi R}{2} C_1 + \frac{\pi R}{2} C_2 \quad (6.7b)$$

($\sigma^* = P / (R\pi)$) from which the coefficients result as

$$C_1 = \frac{15}{2a} \left(1 + \frac{T_1}{\sigma_1} \right) - 8 \frac{T_2}{R\pi\sigma^*} \quad (6.8a)$$

$$C_2 = -\frac{15}{2a} \left(1 + \frac{T_1}{\sigma_1} \right) + 10 \frac{T_2}{R\pi\sigma^*} \quad (6.8b)$$

or by

$$C_1 = \frac{1}{R} \frac{-6.8622 \alpha + 18.1057 \alpha^2 - 22.0173 \alpha^3 + 9.3229 \alpha^4}{1 - \alpha} \quad (6.8c)$$

$$C_2 = \frac{1}{R} \frac{4.1902\alpha - 14.626\alpha^2 + 21.2854\alpha^3 - 9.8117\alpha^4}{1-\alpha} \quad (6.8d)$$

With the improved Green's function the diametral tension specimen was computed again using eq.(5.22). The result is plotted in Fig. 21. It becomes obvious that in this approximation the agreement is significantly better for large α .

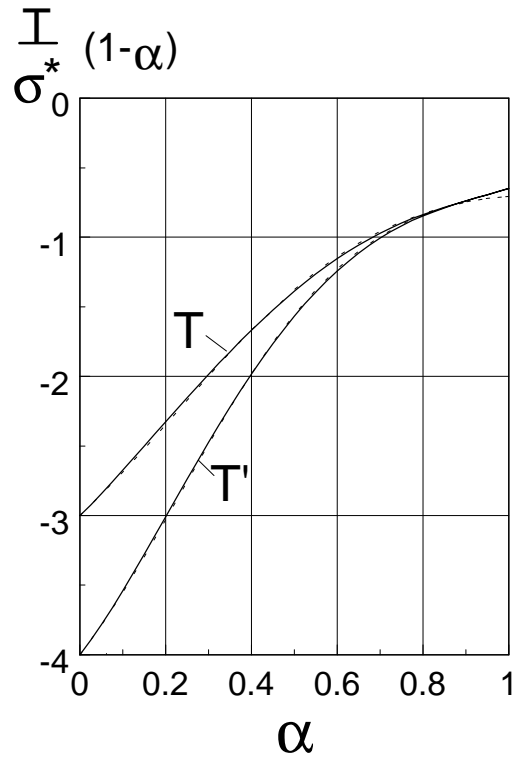


Fig. 21 T-stresses for an internally cracked circular disc, loaded by a couple of diametral forces at the free boundary (see Fig. 11b) estimated with a 2-terms Green's function (dashed curve) compared with results from BCM-computations (solid curve).

7 References

- [1] Larssen, S.G., Carlsson, A.J., *J. of Mech. and Phys. of Solids* **21**(1973), 263-277
- [2] Sumpter, J.D., The effect of notch depth and orientation on the fracture toughness of multipass weldments, *Int. J. Press. Ves. and Piping* **10**(1982), 169-180
- [3] Cotterell, B., Li, Q.F., Zhang, D.Z., Mai, Y.W., On the effect of plastic constraint on ductile tearing in a structural steel, *Eng. Fract. Mech.* **21**(1985), 239-244.
- [4] Leever, P.S., Radon, J.C., Inherent stress biaxiality in various fracture specimen geometries, *Int. J. Fract.* **19**(1982), 311-325.
- [5] Kfoury, A.P., Some evaluations of the elastic T-term using Eshelby's method, *Int. J. Fract.* **30**(1986), 301-315.
- [6] Sham, T.L., The theory of higher order weight functions for linear elastic plane problems, *Int. J. Solids and Struct.* **25**(1989), 357-380.
- [7] Sham, T.L., The determination of the elastic T-term using higher order weight functions, *Int. J. Fract.* **48**(1991), 81-102.
- [8] Fett, T., A Green's function for T-stresses in an edge-cracked rectangular plate, *Eng. Fract. Mech.* **57**(1997), 365-373.
- [9] Fett, T., Munz, D., *Stress intensity factors and weight functions*, Computational Mechanics Publications, Southampton, 1997.
- [10] Wang, Y.Y., Parks, D.M., Evaluation of the elastic T-stress in surface-cracked plates using the line-spring method, *Int. J. Fract* **56**(1992), 25-40.
- [11] Fett, T., T-stress in edge-cracked specimens, FZKA 5802, Forschungszentrum Karlsruhe, 1996.
- [12] Fett, T., Stress intensity factors, T-stress and weight functions for double-edge-cracked plates, FZKA 5838, Forschungszentrum Karlsruhe, 1996.
- [13] Williams, M.L., On the stress distribution at the base of a stationary crack, *J. Appl. Mech.* **24**(1957), 109-114.
- [14] Bückner, H., A novel principle for the computation of stress intensity factors, *ZAMM* **50**(1970), 529-546.
- [15] Irwin, G.R., Analysis of stresses and strains near the end of a crack transversing a plate, *J. Appl. Mech.* **24**(1957), 361-364.
- [16] Gröbner, W., Hofreiter, N., *Integraltafel, Teil 1*, Springer Verlag, Wien New York, 1975.
- [17] Gross, B., Srawley, J.E., Brown, W.F., Stress intensity factors for a single-edge-notched tension specimen by Boundary Collocation of a stress function, NASA Technical Note D-2395, 1965.
- [18] Gross, B., Srawley, J.E., Stress intensity factors for single-edge-notch specimens in bending or combined bending and tension by Boundary Collocation of a stress function, NASA Technical Note D-2603, 1965.
- [19] Newman, J.C., An improved method of collocation for the stress analysis of cracked plates with various shaped boundaries, NASA TN D-6376, 1971.
- [20] Atkinson, C., Smelser, R.E., Sanchez, J., Combined mode fracture via the cracked Brazilian disk test, *Int. J. Fract.* **18**(1982), 279-291

- [21] Awaji, H., Sato, S., Combined mode fracture toughness measurement by the disk test, *J. Engng. Mat. Tech.* **100**(1978), 175-182.
- [22] Fett, T., Mode-II weight function for circular disks with internal radial crack and application to the Brazilian disk test, submitted to *Int. J. Fract./Reports of Current Research*.
- [23] Tada, H., Paris, P.C., Irwin, G.R., *The stress analysis handbook*, Del Research Corporation, St. Louis 1973.
- [24] Rice, J.R., Some remarks on elastic crack-tip stress fields, *Int. J. Solids and Structures* **8**(1972), 751-758.

Appendix

The procedure necessary for the computations addressed in Section 4.2 is illustrated below. A disc geometry may be chosen. Figure A1 explains the principle of superposition for the case of T-stresses. Part a) shows a crack in an infinite body, loaded by a couple of forces P . The T-stress for this case is denoted as T_0 . First we compute the normal and shear stresses along a contour (dashed circle) which corresponds to the disc. We cut out the disc along this contour and apply normal and shear tractions at the free boundary which are identical with the stresses computed before (Fig. A1b).

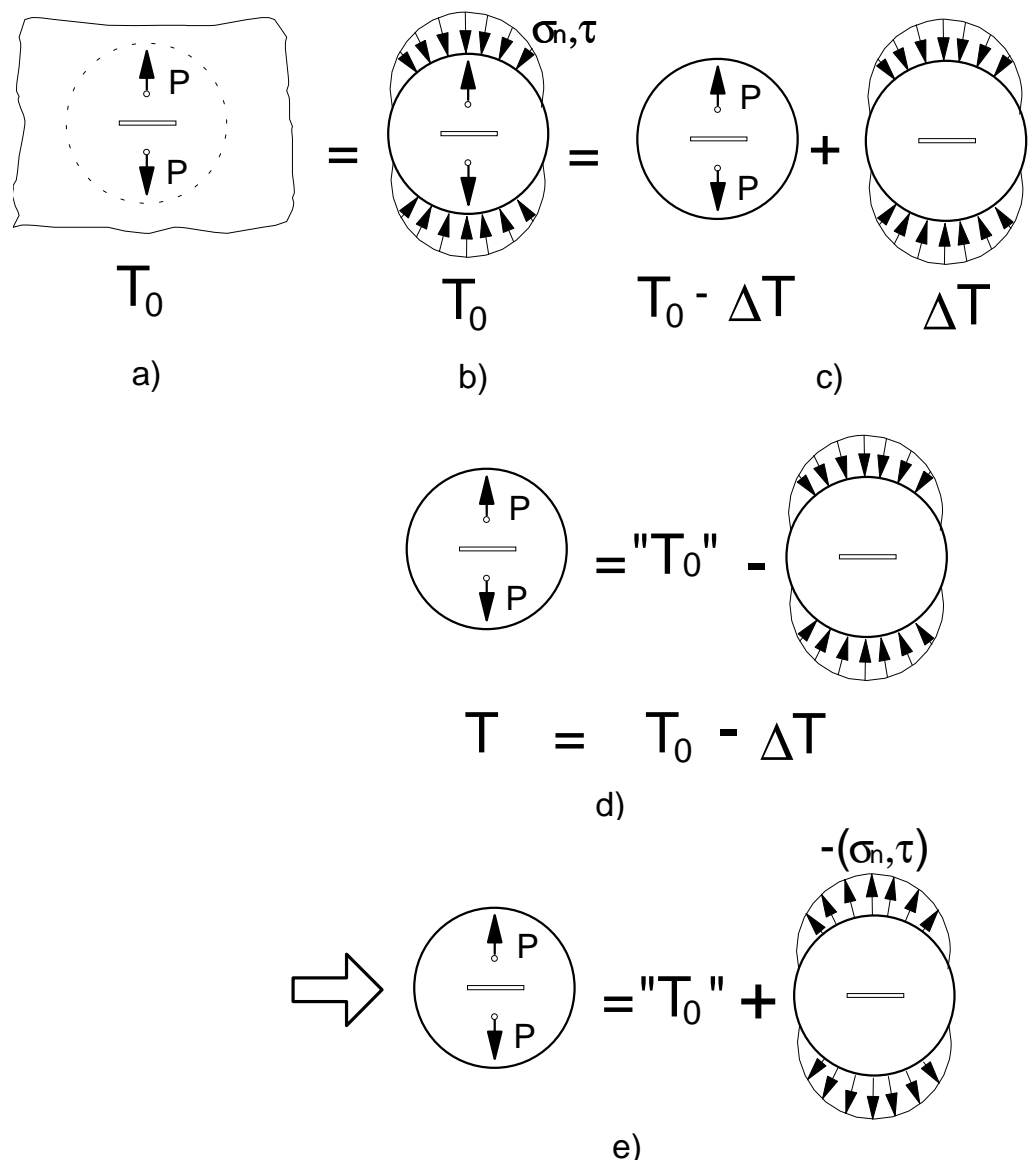


Fig. A1 Illustration of the principle of superposition for the computation of T-stresses for single forces.

The disc loaded by the combination of single forces and boundary tractions exhibit the same T-term T_0 . Next, we consider the situation b) to be the superposition of the two loading cases shown in part c), namely, the cracked disc loaded by the couple of forces (with T-stress $T-\Delta T$) and a cracked disc loaded by the boundary tractions, having the T-term ΔT . As represented by part d), the T-term of the cracked disc is the difference $T=T_0-\Delta T$. If the sign of the boundary tractions is changed, the equivalent relation is given by part e).